

## Functional micropism substrate for organic solar cells

M. Niggemann<sup>a,b,\*</sup>, M. Glatthaar<sup>b</sup>, P. Lewer<sup>a</sup>, C. Müller<sup>c</sup>, J. Wagner<sup>b</sup>, A. Gombert<sup>a</sup>

<sup>a</sup> *Fraunhofer Institut Solare Energiesysteme (ISE), Heidenhofstr. 2, 79110 Freiburg, Germany*

<sup>b</sup> *Freiburger Materialforschungszentrum (FMF), Stefan-Meier-Str. 21, 79104 Freiburg, Germany*

<sup>c</sup> *Institute of Microsystem Technology (IMTEK), Georges-Köhler-Allee 103, 79110 Freiburg, Germany*

Available online 10 February 2006

### Abstract

A novel cell architecture for organic solar cells is presented which is based on a functional micropism substrate. In contrast to the most widely used planar cell architecture with a transparent indium tin oxide (ITO) electrode, the microstructure results in a folded solar cell. Of benefit are the light trapping effect and the substitution of the ITO-electrode by a highly conductive polymer layer with a supporting metal grid. Optical simulations were performed and reveal a gain in absorption in the photoactive layer due to the inclined incidence of radiation and due to the second reflection. Optimal dimensions of the microstructure were calculated by taking the sheet resistivity of the polymer anode and the shading effect of the metal grid into account. The metal grid with a low effective sheet resistance below  $1 \Omega/\square$  was realised by evaporation techniques using the microstructure as a self aligning mask. Investigations on the thin film formation are presented. First micropism solar cells with solar efficiencies comparable to planar ITO-reference solar cells were realised.

© 2005 Elsevier B.V. All rights reserved.

**Keywords:** Light trapping; Substrate; Organic solar cell; Optical modelling

### 1. Introduction

Using organic semiconducting materials in solar cells is a new approach with promising possibilities. The great potential of low cost production combined with mechanical flexibility gives rise to new applications. Due to the relatively simple fabrication process from solution and the mechanical flexibility, the production of organic solar cells by the cost effective roll-to-roll process appears promising. Besides the efficiency and the lifetime, the cost is one of the most important aspects for commercialization of organic solar cells. These preconditions are not fulfilled yet. A promising concept of an organic solar cell is the so-called bulk heterojunction solar cell [1]. The most common donor- and acceptor components are poly-3(hexylthiophene) (P3HT) and [6,6]-phenyl C61-butyric acid methyl ester (PCBM, a C60-derivative) respectively [4]. Standard devices are built up on indium tin oxide (ITO) coated glass or polymer serving as a transparent electrode. Subsequently the organic layers, poly(3,4-ethylenedioxythiophene)-

poly(styrene sulfonate) (PEDOT-PSS), serving as anode and the photoactive blend are deposited from solution. Finally, the aluminium electrode is evaporated on top. One critical point is the price of the rare indium, which is the key component of the most widely used transparent electrode. The efficiency is still limited by the small charge carrier mobilities and the insufficient overlap between the solar spectrum and the absorption of the organic photoactive components. Efficiencies up to 4% are reported for this type of an organic solar cell. We report on a novel cell architecture for organic solar cells based on a micropism substrate. In principle, the geometry can be described by a folded planar solar cell (Fig. 1). This set-up comprises two advantages in comparison to the standard organic solar cell. First, the ITO-electrode is substituted by a highly conductive polymer layer PEDOT:PSS formulation PEDOT CPP 105 D by H.C. Starck) with a supporting metal grid located in the valley of the structure. Second, the micropism structure contributes to an increased light absorption due to a twofold reflection of the incident light. The idea of light trapping structures has been intensively studied for inorganic solar cells and first investigations on light trapping in organic solar cells focussed on diffraction gratings [2,3]. The paper is set out as follows. Optical simulations are presented in order to quantify the expected gain in light absorption. Optimal

\* Corresponding author. Fraunhofer Institut Solare Energiesysteme (ISE), Heidenhofstr. 2, 79110 Freiburg, Germany. Tel.: +49 761 203 4798; fax: +49 761 203 4801.

E-mail address: [Michael.Niggemann@ise.fraunhofer.de](mailto:Michael.Niggemann@ise.fraunhofer.de) (M. Niggemann).

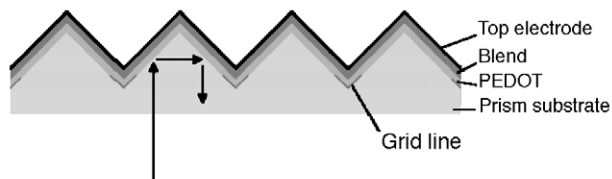


Fig. 1. Cross section of an organic microprism solar cell.

dimensions of the microstructure are then calculated by taking the sheet resistivity of the PEDOT layer and the shading effect of the metal grid into account. Investigations of the metal grid and on the thin film formation are presented. Characteristics of microprism solar cells with efficiencies comparable to planar ITO-reference solar cells are presented and discussed. Finally, approaches for the optimisation of the device with the focus on an improved performance are discussed at the end of this paper.

## 2. Optical simulations

The expected light trapping effect is investigated here. An increased absorption due to the twofold reflection of the incident light can be intuitively assumed. The light absorption in the photoactive layer which is of most importance for solar cells was predicted by simulation calculations. The description of the microprism solar cell using geometrical optics is only valid for structural dimensions larger than several tenths of microns [5]. Since the thickness of a thin film system of several hundred nanometers is much smaller than the coherence length of the incident light, wave optics have to be considered. The calculations of the absorptance in distinct layers were performed by Rigorous Coupled Wave Analysis (RCWA), a method which was implemented for describing near-field phenomena at corrugated interfaces [6–9]. Another approach which is especially suited for thin film devices is the Transfer-matrix formalism [10]. Optical constants are taken for the MDMO-PPV/PCBM system [11] which is comparable to the P3HT/PCBM system with a slight shift in the complex refractive index towards shorter wavelengths. Optical constants for the PEDOT layer were determined for the formulation AI4083 purchased from Bayer and may deviate slightly from the optical constants of the highly conductive PEDOT CPP 105 D which was used in these devices [11]. The thickness of the photoactive layer and the PEDOT layer was 100 nm. Both polarisations of the incident light-transversal electric (TE) and transversal magnetic (TM) were considered.

### 2.1. Angle dependence

The effect of the incident angle of light on the thin film system shall be investigated in detail. The light is incident from a semi-infinite non-absorbing medium with a refractive index of 1.5. The incident angle is varied from 0° (normal incidence) to 80°. In a first approximation the short-circuit current density is calculated from the spectral absorption in the blend layer and the solar spectrum. An internal quantum efficiency of unity is assumed [4]. Calculations for polarised and unpolarised light

are shown in Fig. 2. When the incident angle is increased from normal incidence (0°) up to 80°, the calculated short-circuit current for TE- and TM-polarisation increases up to a certain peak value. For TE-polarisation, the short-circuit current increases up to a maximum of 35.5% at an angle of 60°, whereas for TM-polarisation a maximum increase of 9.8% is calculated at an angle of 45°. For unpolarised light, the peak position can be found at 50° leading to an increase of 18.3%. The reason for an increased charge carrier generation with increasing incident angle can be found in a shift of the spectral absorption in the photoactive layer from short wavelengths towards longer wavelengths (not shown here). The overall photocurrent is increased because of the larger photon flux of the solar spectrum at longer wavelengths. From these initial calculations it can be concluded that inclined incident light on the thin film system should result in an increased short-circuit current in an angular range from 0° to 72° for unpolarised light (see Fig. 2 intersection with dashed line).

#### 2.1.1. Twofold reflection under 45°

The case of normal incident light on the microprism-structure is investigated here. In this constellation, the light is reflected and partially absorbed twice under an angle of 45°. The spectral absorbance of the whole solar cell for a twofold reflection under 45° can be compared with the case of normal incidence on a planar thin film system (see Fig. 3A). An increased absorbance for the microprism cell is observed over the considered spectral range (300 nm–800 nm). The high absorption in TE-polarisation at wavelengths above 600 nm can be traced back to the PEDOT absorbance. Of special interest for the solar cell is the absorption in the photoactive layer (see Fig. 3B). A higher absorption of the whole cell is calculated in TM-polarisation up to a wavelength of 600 nm. The situation changes for the absorption in the photo-active layer. A slightly higher absorbance over the spectral range from 400 nm to 800 nm can be observed for TE-polarisation. From convolution of the spectral absorption in the photoactive layer with the AM1.5 solar spectrum, an increase in absorbance of 55% in TE-polarisation and of 33% in TM-polarisation was calculated relative to the case of normal incident light on a planar solar cell. This leads to an average increase of 44% for

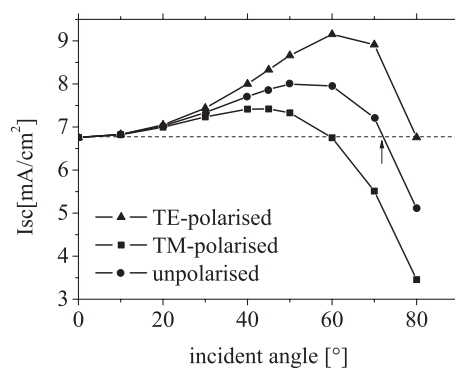


Fig. 2. Calculated angle dependent photocurrent for TE- and TM-polarisation according to an assumed internal quantum efficiency of unity (100 nm PEDOT, 100 nm MDMO-PPV/PCBM-blend, 100 nm aluminium).

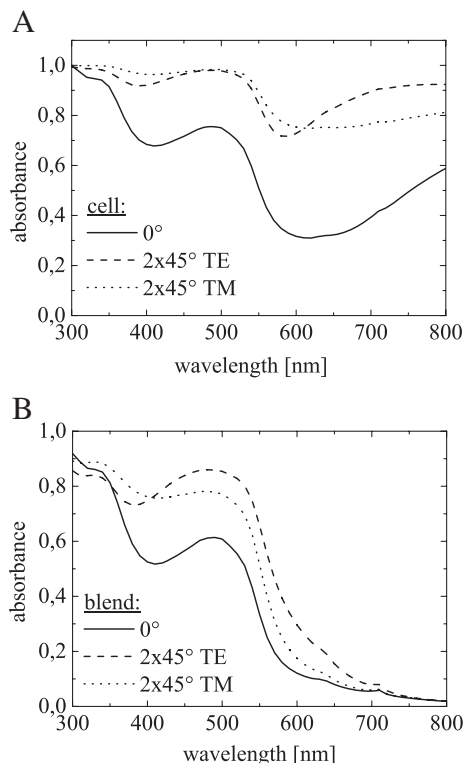


Fig. 3. Calculated spectral absorbance of the whole solar cell A and of the photoactive layer B for a twofold reflection under 45° in TE- and TM-polarisation in comparison to the case of normal incidence on a planar thin film system (100 nm PEDOT, 100 nm MDMO-PPV/PCBM-blend, 100 nm aluminium).

unpolarised light. Optical losses due to shadowing by the microgrid are not taken into account here, but will be considered in the next step.

### 3. Dimensioning of the microstructure

The dimensions of the microstructure strongly affect the efficiency of the solar cell. This becomes obvious as the period of the micropism structure defines the distance of the grid lines. Electrical losses have to be minimized by a sufficiently small distance, whereas the ratio between the lattice distance of the grid and the width of the conducting lines should be as large as possible in order to minimize the shadowing effect. In addition, the metal grid lines have to be sufficiently conductive so that the series resistance is minimized. The following assumptions are made for the calculation of an optimum grid distance. The contribution of the aluminium top electrode and of the gold grid to the series resistance are neglected. The current–voltage characteristics of an infinitesimal small elementary cell with  $V_{oc}=600$  mV,  $I_{sc}=15$  mA/cm<sup>2</sup> and  $FF=0.55$  were taken as input parameters. The electrical losses are calculated in analogy to the calculations presented by Burgelman et al. [12]. In order to determine the optimum lattice distance for a given type of structure, calculations were made for different gridline widths ranging from 2  $\mu$ m up to 40  $\mu$ m and for a sheet resistance varying between  $10^4$   $\Omega/\square$  and  $10^7$   $\Omega/\square$  (Fig. 4). The two competing loss mechanisms

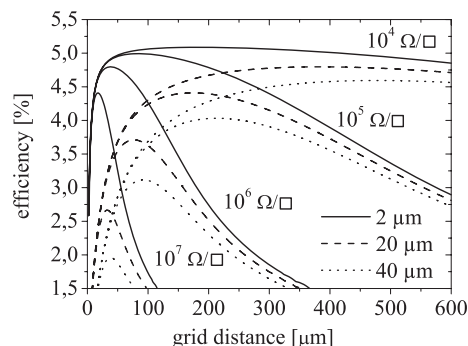


Fig. 4. Calculation of the efficiency depending on the grid distance for different sheet resistances of the PEDOT layer and various widths of the gridlines.

determine the characteristics of the calculations. The steepness of the rising efficiency with increasing grid distance is strongly affected by the shadowing losses caused by the grid lines, whereas the decaying efficiency at larger grid distances is determined by the PEDOT CPP 105 D sheet resistance and therefore by the electrical losses. The geometry of the micropism structure is considered in the calculations by an effectively reduced current density caused by the tilted absorbing surface. It is intuitive that the efficiency of the cell is weakly affected by the grid distance for small widths of gridlines and a small sheet resistance of the PEDOT. To minimise absorption losses in the PEDOT layer, the thickness should range between 80 nm and 120 nm. Assuming a conservative value of  $10^5$   $\Omega/\square$  and a realistic width of the gold grid of 20  $\mu$ m, an optimum grid distance of  $170 \mu\text{m} \pm 50 \mu\text{m}$  (2% deviation from peak efficiency) can be extracted from the calculations. This value corresponds to a period of the micropism structure of  $120 \mu\text{m} \pm 35 \mu\text{m}$ .

## 4. Experimental results

### 4.1. Microstructures

According to the calculations, a suitable period of the prism structure is in the range of  $120 \mu\text{m} \pm 35 \mu\text{m}$ . The experiments presented here were carried out with the 100  $\mu$ m structure which was made by precision micro machining (Forschungs-

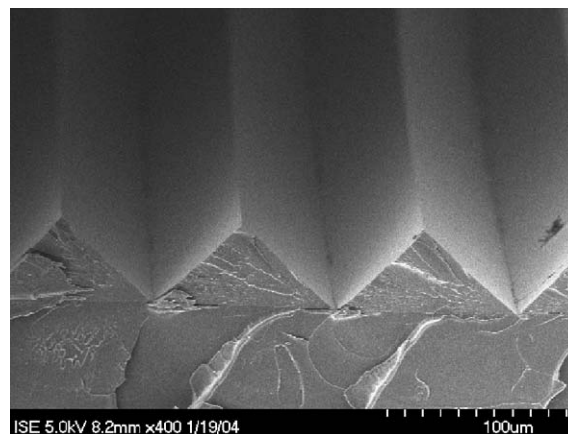


Fig. 5. Cross section of a micropism structure (SEM-image).

zentrum Karlsruhe) and then replicated into an acrylic polymer in a UV-casting process (Fig. 5).

#### 4.2. Microgrid

Organic thin films are deposited on the microstructured polymer substrate by spin coating. Cohesion and adhesion forces lead to an increased thickness of the polymer films in the grooves of the structure which makes the location of the metal grid in the grooves more adequate than on the tips of the structure because the probability of direct shunts between the two metal electrodes is decreased. The grid was realised by combining evaporation techniques under certain incident angles with a lift-off procedure. Here, the microstructure itself is utilized as a self-aligning mask. As a result, a gold grid with a mean width of  $22.5\ \mu\text{m}$  was realized. An effective sheet resistance of a grid with  $100\ \text{nm}$  thick grid lines of  $0.86\ \Omega/\square$  was measured. This is considerably smaller in comparison to the reported value of  $13\ \Omega/\square$  for ITO and therefore advantageous since the less dense network of busbars reduces the shading.

#### 4.3. Thin film deposition

Initial experiments on the deposition of the polymer films on the microprism structure were carried out with spin coating. A homogeneous thickness of the PEDOT and the blend films was assumed over the entire surface of the microstructure for the optical simulation calculations. Of course, a deviation of this ideal case is expected for films deposited on the microprism substrate from solution. The homogeneity of the films was investigated by SEM.

The blend solution, P3HT/PCBM (1:2 by wt. in chlorobenzene), was spin coated on top of the initially coated PEDOT film. The film preparation was done as follows: Prior to the deposition of the organic films, the substrates were dried at  $80\ ^\circ\text{C}$  overnight. The wettability of the surface was enhanced by an oxygen plasma treatment for 10 min. PEDOT CPP 105 D was coated with 2000 rpm for 60 s. The films had to be dried in a vacuum oven for 1 h at  $80\ ^\circ\text{C}$ . The active layer was spun under an argon atmosphere for 60 s with 500 rpm. A complete coating of the microprism structure can be anticipated from SEM investigations.

The thickness of the PEDOT and blend films on the ITO-reference cell were  $\approx 90\ \text{nm}$  and  $\approx 210\ \text{nm}$  respectively. The thickness of the films corresponding to the position on the microprism substrate is shown in Fig. 6. A decay according to an exponential law is obvious. The P3HT/PCBM-blend layer can be divided into 3 regions according to Fig. 7, starting from the valley and ending at the tip at a distance of  $70\ \mu\text{m}$ . The first region is determined by the half width of the grid which is  $10\ \mu\text{m}$  in this case. This area does not contribute to the photocurrent because it is shadowed by the grid. Nevertheless, thicknesses of  $1600\ \text{nm}$  down to  $800\ \text{nm}$  by far exceed the optimum film thickness. In the second region ranging from  $10\ \mu\text{m}$  up to  $35\ \mu\text{m}$ , the film thickness exceeds  $200\ \text{nm}$ . Here, a strong light absorption is expected, however, transport losses

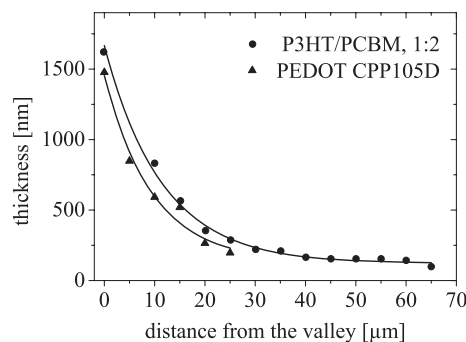


Fig. 6. Measured thickness of the PEDOT and blend thin films on the surface of the microprism structure.

due to recombination will limit the charge extraction. The third region reaches almost to the tip of the pyramid. It is characterised by a film thickness of less than  $200\ \text{nm}$ . Here the microprism structure is expected to be beneficial because transport losses should be small in this region and the twofold reflection should result in an increased absorption. Consequently these optimum conditions are present on 50% of the microprism surface. Therefore the coating process needs further optimisation with the goal of extending the third region. Preliminary experiments with more viscous solutions and higher spin coating velocities showed a sufficiently homogeneous coating on 80% of the surface.

Artifacts caused by the sample preparation process for the SEM investigations prohibited the measurement of the PEDOT film thickness at distances exceeding  $25\ \mu\text{m}$  from the valley. However, the same exponential decay can be assumed and the thickness of the layer can be estimated by extrapolation. Analogous to the blend film, the PEDOT film can also be divided into three zones. The coating of the PEDOT film has to be optimised by extending the third zone with a sufficiently thin film which covers currently approximately 78% of the surface.

#### 4.4. Device characterisation

##### 4.4.1. Absorption measurements

Absorption measurements were carried out in order to verify the optical simulation calculations. Additionally planar polymer samples with the P3HT/PCBM blend (1:2 by wt.) coated on PEDOT were characterised as references. Reflection measurements were made with a Fourier spectrophotometer with an integrating sphere (Bruker IFS 66). Polarisation dependent measurements were performed in order to compare the results with simulation calculations. In TM-polarisation the electric field vector is perpendicular to the microprism grooves while in TE-mounting it is parallel. The optical simulations were carried out with the optical constants for the MDMO-PPV/PCBM blend and will be compared here with the absorption measurements of the P3HT/PCBM blend. The spectral absorption of the microprism cell exceeds the absorption of the planar reference sample (Fig. 8) which is in good agreement with the simulations. TM-polarised light is absorbed more strongly than TE-polarised light over the whole



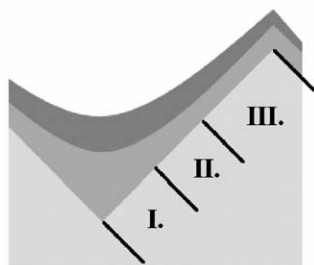


Fig. 7. Sketch of the thin films deposited on the microprism structure divided into three sections.

light spectrum. This is in accordance with the simulations only up to a wavelength of 600 nm. At higher wavelengths the situation changes and the simulations predict a higher absorbance in TE-polarisation than in TM-polarisation. One explanation is a higher absorbance in the PEDOT layer for the simulated case.

#### 4.4.2. Spectral response

The spectral response gives access to the fraction of light which is absorbed in the photoactive layer and contributes to the photocurrent. From the simulation calculations, a higher absorption of the whole solar cell was predicted for TM-polarisation in comparison to TE-polarisation. This was confirmed by the absorption measurements shown before. For the absorption in the photoactive layer, a contrary behaviour was predicted where the absorption of TE-polarised light exceeds the absorption of TM polarised light (see Fig. 3B). Although the measurements shown in Fig. 9 was made on a P3HT/PCBM-blend instead of the simulated MDMO-PPV/PCBM-blend, a slightly increased absorption in TE-polarisation can be confirmed.

#### 4.4.3. Current–voltage characteristics

The current–voltage characteristics was measured under an argon atmosphere using a Steuernagel AM1.5 solar simulator at  $100 \text{ mW/cm}^2$  illumination intensity. As there are still large deviations in the performances of the ITO reference and microprism solar cells, 8 cells of each type were prepared and

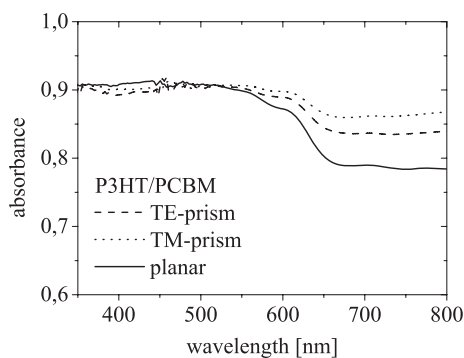


Fig. 8. Polarisation dependent absorbance of a microprism solar cell with a P3HT/PCBM-absorber (1:2 by wt.) in comparison to a coated planar acrylic substrate.

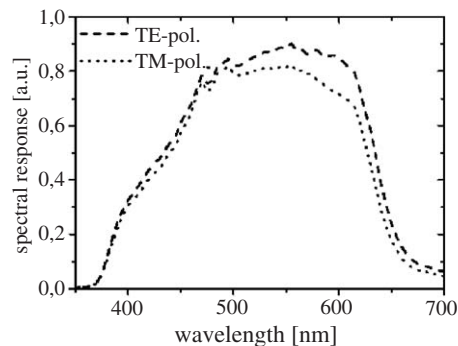


Fig. 9. Spectral response of a microprism solar cell with a P3HT/PCBM-absorber (1:2 by wt.) for TE- and TM-polarised light.

investigated. Exemplar current–voltage characteristics are shown in Fig. 10. By comparing of the characteristics solar cell parameters (not shown here), the following conclusions can be made. The microprism solar cells have significantly smaller open-circuit voltages and fill factors. However, the short-circuit currents  $I_{sc}$  of the microprism cells exceeds the value of the ITO-reference cells. The standard deviations of the microprism solar cell data are significantly larger. It is tempting to explain the increased short-circuit current of the microprism solar cell solely by the light trapping effect of the prism structure. But an increased current together with a reduced fill factor can also be caused by an increased film thickness which is evident on 50% of the area. Hence, a superposition of both effects is expected. From the measured current–voltage characteristics of cell specimens, an increased slope under applied negative voltage can be observed for the microprism solar cells in Fig. 10 in comparison to the ITO reference cells. This behaviour can be explained by a shunt resistance, as it can be observed in the dark, too. The origin of the electrical shunts was investigated by lock-in thermography, a method which is already established for silicon solar cells. Strong evidence for the presence of the electrical shunts predominantly on the tips of the microprisms were found. Although the efficiency of 1.1% is far below the best published results for an ITO-based device, it is a promising result since the parameters have not been optimised yet.

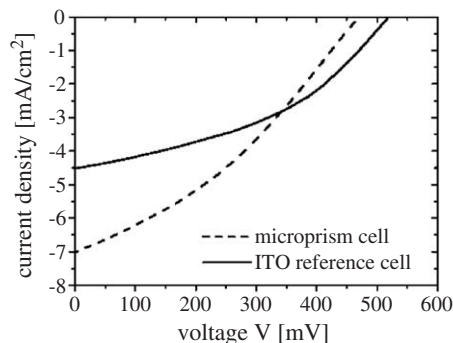


Fig. 10.  $IV$ -curve of a microprism organic solar cell and an ITO reference cell. Microprism cell:  $V_{oc}=455 \text{ mV}$ ,  $I_{sc}=7 \text{ mA/cm}^2$ ,  $FF=0.35$ ,  $\eta=1.1\%$ .

## 5. Summary and conclusions

Optical simulations reveal two effects which contribute to an increased light absorption in the photoactive layer. First, the inclined incident angle with a maximum absorption at  $50^\circ$  for unpolarised light and second the additional reflection at the opposite surface of the prism. In comparison to a planar solar cell with a 100 nm thick absorber (MDMO-PPV/PCBM), a twofold reflection under  $45^\circ$  enhances the light absorption by 44% with respect to the solar spectrum (unpolarized light, shadowing losses by the grid are not taken into account). The dimensions of the microstructure have a strong influence on the solar cell efficiency. The two competing mechanisms are the ohmic losses in the polymer anode (PEDOT) and the shadowing losses caused by the microgrid. For a low sheet resistance of PEDOT of approximately  $10^5 \Omega/\square$  and a 20  $\mu\text{m}$  wide gold grid the optimum period of the prism structure is  $120 \mu\text{m} \pm 35 \mu\text{m}$ . The microgrid was realised by combining evaporation techniques under certain incident angles with a lift-off procedure. A sheet resistance of the gold grid of  $0.86 \Omega/\square$  was measured for 100 nm thick and 22.5  $\mu\text{m}$  wide gridlines on a prism substrate with a period of 100  $\mu\text{m}$ . The homogeneity of spin-coated blend and PEDOT films on the micropism structure is not optimized yet. Preliminary experiments showing sufficiently thin films on 80% of the surface appear promising. However the geometry of the microstructure has to be modified, too. The insufficient wetting at the sharp tips is expected to cause the electrical shunts and shall therefore be improved by rounded tips in future experiments. First micropism solar cells were built with efficiencies comparable to planar reference solar cells on ITO substrates. Nevertheless, the current–voltage characteristics differed. The open-circuit voltage and fill factor of the reference cells was significantly higher. This was compensated by a higher short-circuit current of the micropism cell which is attributed to the thicker and therefore better absorbing photoactive layer as well as by the light trapping effect of

the micropisms. Absorption measurements on micropism solar cells as well as measurements of the spectral response showed a similar behaviour as was predicted from optical calculations.

Although the ITO-electrode was substituted, the generation of the microgrid by evaporation techniques in combination with a lift-off procedure might still be a bottleneck for low cost production. Alternative methods for the generation of the microgrid need to be developed.

## Acknowledgements

This work was supported by the Bundesministerium für Bildung und Forschung (BMBF) under contract number 01SF0119.

## References

- [1] S.E. Shaheen, C.J. Brabec, N.S. Sariciftci, F. Padinger, T. Fromherz, J.C. Hummelen, *Appl. Phys. Lett.* 78 (6) (2001) 841.
- [2] L.S. Roman, O. Inganäs, T. Granlund, T. Nyberg, M. Svensson, M.R. Andersson, J.C. Hummelen, *Adv. Mater.* 12 (3) (2000) 189.
- [3] M. Niggemann, M. Glatthaar, A. Gombert, A. Hinsch, V. Wittwer, *Thin Solid Films* 451–452 (2004) 619.
- [4] P. Schilinsky, C. Waldauf, C.J. Brabec, *Appl. Phys. Lett.* 81 (20) (2002) 3885.
- [5] E. Hecht, *OPTIK*, third edition, Addison-Wesley Publishing Company, 1974.
- [6] M.G. Moharam, T.K. Gaylord, *J. Opt. Soc. Am.* 72 (10) (1982) 1385.
- [7] M.G. Moharam, T.K. Gaylord, *J. Opt. Soc. Am. A, Opt. Image Sci. Vis.* 71 (1981) 811.
- [8] P. Lalanne, G.M. Morris, *J. Opt. Soc. Am. A, Opt. Image Sci. Vis.* 13 (4) (1996) 779.
- [9] P. Lalanne, M.P. Jurek, *J. Mod. Opt.* 45 (7) (1998) 1357.
- [10] H. Hoppe, N. Arnold, N.S. Sariciftci, D. Meissner, *Sol. Energy Mater. Sol. Cells* 80 (1) (2003) 105.
- [11] H. Hoppe, N.S. Sariciftci, D. Meissner, *Mol. Crystals Liq. Crystals* 385 (2002) 233.
- [12] M. Burgelman, A. Niemegeers, *Sol. Energy Mater. Sol. Cells* 51 (2) (1998) 129.